Hydrodynamics of Pair-Annihilating Disclinations in Sm*C* Films

D. Svenšek* and S. Žumer

Department of Physics, University of Ljubljana, Jadranska 19, SI-1000 Ljubljana, Slovenia

(Received 27 July 2002; published 14 April 2003; publisher error corrected 15 May 2003)

The pair annihilation of smectic *c*-director defects with winding numbers ± 1 in a freestanding Sm*C* film as a representative of the *XY* model is studied numerically, considering a full coupling of orientational degrees of freedom and hydrodynamics. A reduction of the annihilation time compared to the nonhydrodynamic treatment is observed. It is demonstrated that the $+1$ disclination moves considerably faster than the -1 one primarily due to hydrodynamic flow, weakly assisted also by elastic anisotropy. The stress tensor terms and material parameters relevant for this effect are identified.

DOI: 10.1103/PhysRevLett.90.155501 PACS numbers: 61.30.Jf, 47.15.Gf, 61.30.Dk, 68.15.+e

Topological defects represent a universal link between completely different areas of physics involving broken symmetries, such as cosmology, particle physics, and condensed matter physics. In particular, defects play a decisive role in any phase transition, since in the late stages the ordering is governed exclusively by the dynamics of the defects created at the transition. Lately, the aim towards the exploitation of the universality of defects has been experienced in this area, motivating the research of laboratory-friendly condensed matter systems such as liquid crystals or superfluid helium to yield knowledge in other areas of physics (e.g., cosmic strings), where no experiments are possible [1–4]. Experimentally, one convenient liquid crystal system is the freestanding smectic-*C* (Sm*C*) thin film. In the Sm*C* phase, the average direction of the molecules, specified by the unit nematic director, is tilted with respect to the smectic layer normal. The projection of the director onto the layer plane, a two-dimensional vector **c**, is one of the Sm*C* phase order parameters to be addressed in this Letter. Topological defects in the **c** field are disclinations with integer winding numbers, i.e., vortices.

Until now, significant work has been done on the hydrodynamics of defects in nematics [5–7]. There we have studied [7] the influence of reorientation-induced hydrodynamic flow on the pair annihilation of straight $\pm 1/2$ disclination lines. A recent experiment by Bogi *et al.* [8] is presumed to be capable of testing the predictions of Refs. [6,7]. It must be stressed, however, that the order parameters of the Sm*C* thin film and the nematic are fundamentally different, and it is the Sm*C* thin film system — within the restrictions given below — rather than the nematic that is a representative of the *XY* model. Therefore, we believe that the Sm*C* dynamics has a wider range of applicability, which essentially motivates its analysis. Besides, in the nematic tensorial case the dynamics of the strength 1 (or -1) vortex cannot be followed as it is unstable — it is decomposed into a pair of repelling strength $1/2$ (or $-1/2$) disclinations.

A direct motivation for this work has been an experiment on the pair annihilation of vortices in Sm*C* thin films by Link *et al.* [9]. Apart from Pleiner's phenomenological description of forces on a single defect [10], there have been no theoretical hydrodynamic studies of vortices in Sm*C* systems. In this Letter, we set the scene for an adequate description of defect dynamics in Sm*C* films. Then we show that the pair annihilation of strength ± 1 vortices (Fig. 1) is accompanied by strong flow, which speeds up the process as compared with the model situation without the flow and, assisted by the elastic anisotropy, gives rise to asymmetry in defect speeds.

The starting point is the hydrodynamic theory of Sm*C* liquid crystals proposed by Carlsson *et al.* [11,12]. It assumes a constant smectic layer thickness and a constant average tilt of the molecules. In order to describe the structure of the vortices, however, at least the constraint of constant tilt has to be relaxed, i.e., a slight generalization of the theory is necessary. At the same time, a substantial simplification will be made; that is, a system with variations only in two dimensions and with straight smectic layers will be assumed, eliminating the layer normal degree of freedom completely and fixing it to

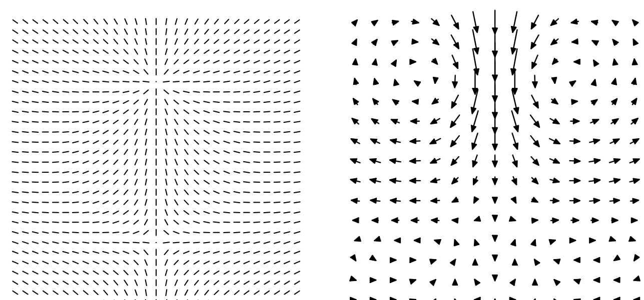

FIG. 1. Left: radial-hyperbolic pair of annihilating ± 1 disclinations in **c** field (the grid has been coarsened for clarity; only the central region of the mesh is shown). Vector heads have been omitted for legibility; yet there is no ambiguity, since in the absence of any external fields the system is invariant under a global transformation $\mathbf{c} \to -\mathbf{c}$. Right: flow velocity field (same region as on the left diagram, coarser still). The $+1$ defect is subject to strong advection, as opposed to the -1 one.

$\hat{\mathbf{e}}_z$. Experimentally, Sm*C* thin films are much closer to the two-dimensional theoretical description than the nematics [6,7], where the disclination lines can curve and fluctuate. Because of the thin film geometry, two spatial variables x and y, with $\nabla = \hat{\mathbf{e}}_x \partial_x + \hat{\mathbf{e}}_y \partial_y$, and a planar flow $\mathbf{v} = v_x \hat{\mathbf{e}}_x + v_y \hat{\mathbf{e}}_y$ are assumed. We have thus reduced the Sm*C* thin film system to the *XY* model. It can be shown by a brief inspection that, under these assumptions, the constant-tilt Sm*C* theory [11,12] reduces to the Ericksen-Leslie (EL) theory of the nematic liquid crystal exactly. In addition, the modulus of $\mathbf{c}$, corresponding to the sine of the tilt angle, will be allowed to vary [10]. Thus, in the center of the defect $\mathbf{c}$ vanishes, and the system converts locally to the Sm*A* configuration.

The free energy density $f(\mathbf{c}, \nabla\mathbf{c})$ is expressed as

$$f = \tfrac{1}{2}Ac^2 + \tfrac{1}{4}Cc^4 + \tfrac{1}{2}B_1(\nabla \times \mathbf{c})^2 + \tfrac{1}{2}B_2(\nabla \cdot \mathbf{c})^2. \quad (1)$$

The first two terms describe the Sm*A* to Sm*C* phase transition, with the equilibrium modulus $c_0 = \sqrt{-A/C}$. In the original constant-tilt description [11], the elastic part involves nine coefficients, which for fixed and straight smectic layers reduce to the bend (B_1) and splay (B_2) coefficients only. On account of the variable modulus of $\mathbf{c}$, B_1 and B_2 are tilt independent, while additional elastic terms should be added to (1). Their relevance is limited to regions where the modulus of $\mathbf{c}$ varies, i.e., to the defect cores. In order to keep the number of material parameters as low as possible, these terms will not be included. Nevertheless, we do retain the splay-bend elastic anisotropy, which in Sm*C* liquid crystals can be large due to spontaneous polarization effects [13–15]. Neglecting surface terms, Eq. (1) represents a consistent omission of the additional elastic terms.

The Euler-Lagrange equation for the free energy functional $F = \int dV f(\mathbf{c}, \nabla\mathbf{c})$ gives the homogeneous and elastic part of the generalized force acting on the vector $\mathbf{c}$:

$$h_i = -(A + Cc^2)c_i + B_1 \partial_j^2 c_i + (B_2 - B_1)\partial_i \partial_j c_j. \quad (2)$$

The elastic stress tensor is obtained from (1) as

$$\sigma_{ij}^e = -\frac{\partial f}{\partial(\partial_i c_k)} \partial_j c_k. \quad (3)$$

Originally, the theory [12] involves 20 viscous terms, of which only the standard Leslie terms are left in the actual limit of lateral flow, straight smectic layers, and no gradients in the direction of the layer normal. Hence, the viscous stress tensor is

$$\begin{aligned}\sigma_{ij}^v = {} & \tfrac{1}{2}\gamma_1(N_i c_j - c_i N_j) + \tfrac{1}{2}\gamma_2(N_i c_j + c_i N_j) \\ & + \alpha_1 c_k c_l \mathsf{A}_{kl} c_i c_j + \alpha_4 \mathsf{A}_{ij} + \alpha_5 c_i \mathsf{A}_{jk} c_k \\ & + \alpha_6 \mathsf{A}_{ik} c_k c_j, \end{aligned} \quad (4)$$

and the generalized viscous force on the vector $\mathbf{c}$ is

$$-h_i^v = \gamma_1 N_i + \gamma_2 \mathsf{A}_{ij} c_j, \qquad N_i = \dot{c}_i + \mathsf{W}_{ij} c_j, \quad (5)$$

where $\gamma_1 = \alpha_3 - \alpha_2$ (rotational viscosity), $\gamma_2 = \alpha_3 + \alpha_2$, with $\dot{\mathbf{c}} = \partial\mathbf{c}/\partial t + (\mathbf{v} \cdot \nabla)\mathbf{c}$, and $\mathsf{A}_{ij} = \frac{1}{2}(\partial_i v_j + \partial_j v_i)$, $\mathsf{W}_{ij} = \frac{1}{2}(\partial_i v_j - \partial_j v_i)$. Again, new terms arising from the dissipation related to the time derivative of the modulus of $\mathbf{c}$ could, in principle, have been added to (4) and (5), but in order to limit the set of viscous parameters to the standard Leslie coefficients only, they were left out. Unlike the viscosities in Ref. [12], the α's in (4) and (5) are tilt independent.

By allowing the modulus of $\mathbf{c}$ to vary in Eqs. (1)–(5), we make a natural generalization of the EL description to the case of the nonunit vector order parameter. Hereby we automatically recover the correct tilt dependence of the forces, which in Refs. [11,12] must be regulated by tilt-dependent coefficients, suggested by symmetry arguments. For nematics, in contrast, only the tensorial description will provide the proper dependence of the material parameters on the degree of order/biaxiality. Hence, it is exactly the modeled Sm*C* film system rather than the nematic to which the EL theory applies rigorously (within the restrictions considered).

The equation of motion for the vector $\mathbf{c}$ reads briefly

$$\mathbf{h} + \mathbf{h}^v = 0. \quad (6)$$

The generalized Navier-Stokes equation within the low-Reynolds-number approximation [7,16,17] reads

$$\rho \frac{\partial v_i}{\partial t} = -\partial_i p + \partial_j(\sigma_{ji}^v + \sigma_{ji}^e), \quad (7)$$

with the density ρ and the stress tensors given in (4) and (3). Usually, the steady state approximation is also made, omitting the time derivative term from Eq. (7) [7,16,17]. The pressure field p is controlled by the incompressibility condition $\partial_i v_i = 0$.

Equation (6) and the stationary version of Eq. (7) can both be cast in dimensionless form by introducing a characteristic length, e.g., the correlation length $\xi = \sqrt{B_0/(A + 3Cc_0^2)}$, typically a couple of nanometers, and a characteristic time $\tau = \gamma_1 \xi^2 / B_0$, where $B_0 = (B_1 + B_2)/2$. The time τ is the characteristic relaxation time of the $\mathbf{c}$ deformations on the length scale of ξ or, equivalently, the dynamic time of the modulus of $\mathbf{c}$, typically tens of nanoseconds. In the following, dimensionless quantities will be used, i.e., $r \leftarrow r/\xi$ for length, $t \leftarrow t/\tau$ for time, and $v \leftarrow v\tau/\xi$ for the velocity. Doing so, the material parameters enter the equations only through ratios given below.

The coupled partial differential equations (6) and (7) are solved using finite difference discretization on a staggered grid [18], p. 331; see [7] for an outline. The calculations were done on a square mesh, consisting of a fine homogeneous mesh of 80×80 points in the center containing both defects, and an inhomogeneous grid with increasing spacing around it to yield the total of 140×140 points. The velocity was set to zero at the boundary.

In order to simulate a bulk system, the defect separation was small compared to the size of the computational area (the ratio of the two was 3/20) and the derivatives of the order parameter normal to the boundary were set to zero.

A generic set of viscous parameters in (4) and (5) was used, corresponding to the Leslie coefficients of the nematic substance 4-methoxybenzyliden-4′-butylanilin [19], p. 231, with the relevant ratios $\gamma_2/\gamma_1 \approx -1.0$, $\alpha_1/\gamma_1 \approx 0.085$, $\alpha_4/\gamma_1 \approx 1.1$, $\alpha_5/\gamma_1 \approx 0.61$, $\alpha_6/\gamma_1 \approx -0.42$. The Landau coefficients A, C, and the elastic constants in (1) were in the ratios of $A\xi^2/B_0 \approx -0.50$, $C\xi^2/B_0 \approx 2.0$ (yielding equilibrium tilt value of 30°), with the correlation length $\xi \approx 2.4$ nm. The time $\tau \approx 88$ ns completes the set of parameters.

Early stages of the annihilation process exhibit a dependence on the initial configuration (Fig. 2). Starting with the equilibrium structure of two fixed defects, a transition period exists, during which the static equilibrium configuration is changing to a dynamic one [7,20]. The transient can also be interpreted in terms of an effective mass of the defect due to the distortion of the **c** field caused by the defect motion [10]. To suppress it, a scaling technique was used to obtain the starting configuration, based on the self-similarity of the **c** field, attained when far away from the start but still in the limit where the defect separation R is large compared to ξ. The defects were left to annihilate to half the initial separation, followed by a rescaling of the **c** field to the initial defect separation and a short simulation run to equilibrate the tilt. This starting configuration is considered as a useful approximation—in reality, the scaling regime, where $R \propto (t_0 - t)^{1/2}$ would hold, is approached only at very large distances due to logarithmic corrections [21].

First we focus on the hydrodynamic effects on the pair annihilation in the one elastic constant approximation, $B_1 = B_2$. Significant asymmetry in the defect motion and reduction of the annihilation time as compared to the nonhydrodynamic treatment is observed (Fig. 3), very similar to the case of $\pm 1/2$ defects in nematics [7]. It is possible to understand this easily by inspecting the flow-driving terms in the stress tensor: the elastic terms (3) and the γ_1 and γ_2 terms in the viscous stress (4). The main flow effect appears to be the advection, i.e., the hydrodynamic transport, which is discussed in the following. The viscous influence on **c** comes second, though it is not negligible.

If one performs a reflection of the **c** vectors in the line joining the defects, the winding number of the defects is reversed, but the order parameter dynamics stays the same in the one elastic constant approximation. To recover the original configuration (up to an irrelevant global minus sign), a π rotation of the sample around an axis perpendicular to the film through the middle point between the defects is required. Performing the reflection on the stress tensor terms mentioned, one can verify that the γ_1 term is antisymmetric (provided that

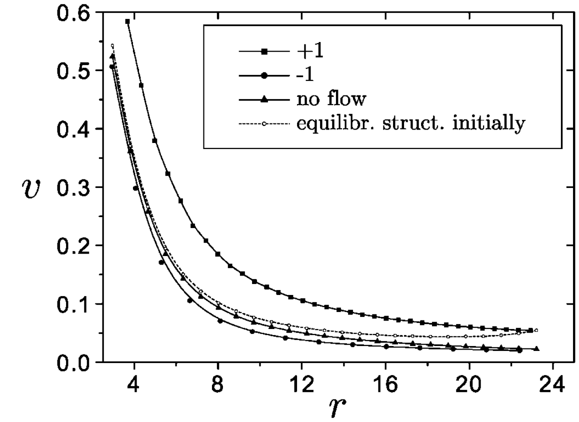

FIG. 2. Velocity of the defects (relative to $\xi/\tau \approx 27$ nm/μs) vs interdefect distance, one elastic constant. The $+1$ defect is strongly sped up by the flow, the -1 is slightly slowed down (there the flow is opposite to its motion, Fig. 1). Starting with an equilibrium configuration of fixed defects, a nonmonotonic behavior is observed (dashed line).

the flow is generated by this term only and that the α_1, α_5, and α_6 terms are neglected) and the γ_2 term has no definite symmetry, while the elastic stress is symmetric by definition. This means that the flow generated by the elastic stress is symmetric with respect to the rotation about the perpendicular axis, while the one driven by the γ_1 viscous term is antisymmetric. In other words, the elastic stress driven flow carries the defects symmetrically toward each other [7], as in this way the free energy is reduced. Thereby it contributes to the speedup of the process. On the other hand, the flow driven by the γ_1 term carries both defects with equal speeds and in the same direction [7], downward in Fig. 1. This is the main reason

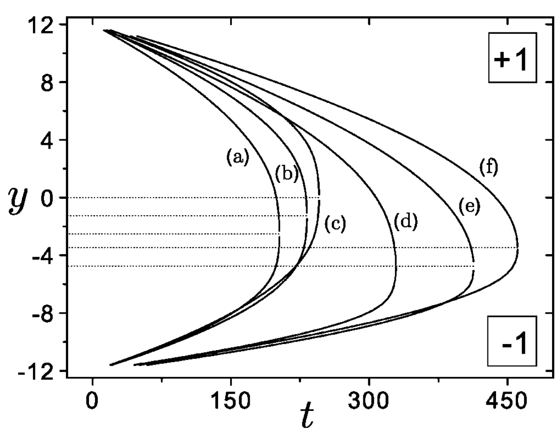

FIG. 3. Position of the defects vs time, measured from the initial middle point between the defects. The cases with one elastic constant: (*a*) RH (Fig. 1) and (*b*) TH defect pair, (*c*) the case without hydrodynamics, (*d*) RH pair with the γ_1 coefficient doubled. Combined effect of flow and elastic anisotropy, with the average elastic constant B_0 fixed: (*e*) $B_1/B_2 = 5$ (RH), (*f*) $B_2/B_1 = 5$ (TH). Length and time are scaled by $\xi \approx 2.4$ nm and $\tau \approx 88$ ns, respectively.

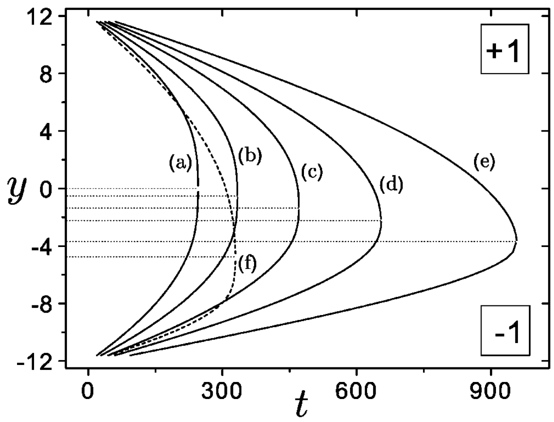

FIG. 4. The effect of elastic anisotropy (without the hydrodynamics). The ratio of elastic constants is (*a*) 1, (*b*) 2, (*c*) 4, (*d*) 8, and (*e*) 16; B_0 is kept constant. (*f*) For comparison, the hydrodynamic one elastic constant case with γ_1 doubled is shown.

for the $+1$ defect moving faster. What is more, on this basis it can be understood why the flow near the $+1$ defect is much stronger as compared with that near the -1 defect (Fig. 1): in the first case the flow fields from the two sources are added, while in the second they combine destructively. Finally, the velocity magnitude of both flows relative to the speed of defect motion just due to reorientation of **c** is proportional to γ_1/α_4.

The asymmetric γ_2 viscous term complicates the situation. It is this term that is mainly responsible for the different flow effect in case of different defect pairs [e.g., radial-hyperbolic (RH) vs tangential-hyperbolic (TH, a homogeneous $\pi/2$ rotation of **c** on the RH structure), Figs. 3*a* and 3*b*], since the γ_1 and the elastic terms are left unchanged by the homogeneous rotation, and so is the viscous torque on **c**, given by the γ_1 part of the viscous force (5). The passive viscous terms (α_1, α_5, α_6) need not be discussed in the qualitative picture.

The asymmetry of defect motion arises also from elastic anisotropy. In Sm*C* chiral systems, this can be large due to **c** deformation induced gradients of polarization **P** and thus appearance of an electric charge, $e = -\nabla \cdot \mathbf{P}$. The polarization vector lies in the smectic plane, usually perpendicularly to **c**, thus increasing the bend elastic constant [13]. However, in very thin systems surface polarization might dominate [15], strengthening the splay rigidity [14]. The annihilation processes at different ratios of the elastic constants are presented in Fig. 4, while the combined effect of the flow and the anisotropy is demonstrated in Fig. 3, curves (*e*) and (*f*). Without the flow, inverting the ratio and correspondingly changing the structure, RH $\leftrightarrow$ TH, does not change the dynamics, so it is enough to consider one type of elastic anisotropy only.

To conclude, under the restrictions mapping the Sm*C* thin film system to the *XY* model, we have reduced the Sm*C* dynamic theory [11,12] to the EL theory. We have demonstrated that the latter, naturally generalized to the variable modulus of the vector order parameter, exactly describes the model system containing vortices. Numerically, we have shown that the influence of hydrodynamics depends primarily on the ratio of rotational and translational viscosity γ_1/α_4, controlling the hydrodynamic acceleration of the process and the defect speed asymmetry, and on the ratio γ_2/α_4, breaking invariance upon configurations, differing only by a homogeneous rotation of the vector **c**. To a lesser extent, the motion asymmetry is contributed to also by the elastic anisotropy.

This work was supported by the Slovenian Office of Science (P0-0503-1554) and U.S.–Slovene NSF Joint Fund (9815313).

*Corresponding author.
Email address: daniel@fiz.uni-lj.si

[1] W. H. Zurek, Nature (London) **317**, 505 (1985).
[2] H.-R. Trebin, Liq. Cryst. **24**, 127 (1998).
[3] I. Chuang, R. Durrer, N. Turok, and B. Yurke, Science **251**, 1336 (1991).
[4] T. W. B. Kibble, Physica (Amsterdam) **369C**, 87 (2002).
[5] J. I. Fukuda, Eur. Phys. J. B **1**, 173 (1998).
[6] G. Tóth, C. Denniston, and J. M. Yeomans, Phys. Rev. Lett. **88**, 105504 (2002).
[7] D. Svenšek and S. Žumer, Phys. Rev. E **66**, 021712 (2002).
[8] A. Bogi, P. Martinot-Lagarde, I. Dozov, and M. Nobili, Phys. Rev. Lett. **89**, 225501 (2002).
[9] D. R. Link, A. Tewary, G. Natale, V. Ginzburg, J. E. Maclennan, L. Radzihovsky, and N. A. Clark (unpublished).
[10] H. Pleiner, Phys. Rev. A **37**, 3986 (1988).
[11] T. Carlsson, I. W. Stewart, and F. M. Leslie, Liq. Cryst. **9**, 661 (1991).
[12] T. Carlsson, F. M. Leslie, and N. A. Clark, Phys. Rev. E **51**, 4509 (1995).
[13] C. Y. Young, R. Pindak, N. A. Clark, and R. B. Meyer, Phys. Rev. Lett. **40**, 773 (1978).
[14] C. Rosenblatt, R. Pindak, N. A. Clark, and R. B. Meyer, Phys. Rev. Lett. **42**, 1220 (1979).
[15] D. R. Link, J. E. Maclennan, and N. A. Clark, Phys. Rev. Lett. **77**, 2237 (1996).
[16] D. Svenšek and S. Žumer, Liq. Cryst. **28**, 1389 (2001).
[17] D. Svenšek and S. Žumer, Continuum Mech. Thermodyn. **14**, 231 (2002).
[18] C. A. J. Fletcher, *Computational Techniques for Fluid Dynamics* (Springer-Verlag, Berlin, 1988), Vol. II.
[19] P. G. de Gennes and J. Prost, *The Physics of Liquid Crystals* (Clarendon Press, Oxford, 1995).
[20] L. M. Pismen, *Vortices in Nonlinear Fields* (Oxford University Press, Oxford, 1999).
[21] B. Yurke, A. N. Pargellis, T. Kovacs, and D. A. Huse, Phys. Rev. E **47**, 1525 (1993).